Thermomechanical Characterization of High Temperature SMA Actuators

Parikshith K. Kumar[a] , Dimitris C. Lagoudas[b], Kevin J. Zanca[c], Magdalini Z. Lagoudas[d]

[a] Graduate Student, Aerospace Engineering, Texas A & M University, College Station, Texas 77843
[b] John and Bea Slattery Chair, Professor, Aerospace Engineering, Texas A & M University, College Station, Texas 77843
[c] Conveyance Engineering, Schlumberger, Sugarland, Texas 77478-2899
[d] Associate Director, Spacecraft Technology Center, Texas A & M University, College Station, Texas 77843

ABSTRACT

The focus of this paper is the study and thermomechanical characterization of High Temperature Shape Memory Alloys (HTSMAs) at different stress levels and temperatures ranging from 300 to 500°C. The stability of the material response under cyclic actuation is also investigated. The observations deduced from the tests are presented in detail. In order to investigate the above issues a $Ti_{50}Pd_{40}Ni_{10}$ HTSMA was used. The alloy was fabricated by a vacuum arc melting technique, followed by casting and hot rolling. A high temperature experimental setup was developed on a load frame to test the material at high temperatures under constrained actuation conditions. Certain key observations on the material response, in terms of recoverable strains under various applied total strains and actuation stress levels, and cyclic thermomechanical behavior are presented.

Keywords: Thermomechanical characterization, High Temperature, HTSMA, TiPdNi.

1. INTRODUCTION

Shape Memory Alloys (SMAs) have been the focus of study among researchers for the past several decades due to their unique Shape Memory Effect (SME) and pseudoelastic properties, and have been increasingly used in a wide range of devices and applications due to their high energy density [1,2]. The growing efforts to utilize this material behavior for potential commercial applications is observed in the emerging diversification of this field into ferrous, magnetic, high temperature and biocompatible shape memory alloys [1, 3- 5]. This diversification is achieved by creating innovative alloy materials that exhibit unique and necessary properties and are capable of operating under different control conditions such as thermal, mechanical and magnetic fields. Addition of ternary elements such as Hafnium, Palladium or Zirconium to conventional binary NiTi can shift the transformation temperatures above 100°C to create a new range of HTSMAs with transformation temperatures as high as 1000 °C [4, 6, 7]. HTSMAs with actuation temperatures greater than 100°C could provide solutions to a whole range of high temperature applications in the automotive, aircraft and oil industries [8, 9].

Several binary and ternary HTSMAs have been investigated over the last decade by various researchers. The SME behavior of these materials has been studied at different temperatures under zero stress condition. Most of the mechanical tests conducted earlier were performed at room temperature [6]. Recent studies on high temperature alloys were carried out under silicon oil bath or in vacuum conditions [10, 11]. Brittleness, poor ductility and poor SME have been observed in binary HTSMAs such as NiAl and TiPd with increased testing temperatures [10, 12]. Different techniques have been adopted to improve the behavior of these alloys, which include alloying with additional elements, thermo mechanical treatments, and precipitation hardening techniques [11, 13, 14]. NiTiPd of different compositions have shown improved SME behavior after thermomechanical treatments or precipitation hardening [11, 14]. The pseudoelastic behavior in TiPdNi alloys has also been investigated by several researchers [15-17]. Due to the high transformation temperatures (greater than 100°C), effects such as oxidation, recovery and recrystallization in grains and its influence on the materials behavior become critically important [18-21]. In TiPdNi HTSMAs, softening, recovery and recrystallization at temperatures close to austenitic start (A_s) have been reported based on Transmission Electron Microscopy (TEM), Differential Scanning Calorimetry (DSC) and hardness measurements [18-21].

This work focuses on the thermo-mechanical characterization of a $Ti_{50}Pd_{40}Ni_{10}$ alloy, investigating its performance for usage as a potential actuator in a high temperature environment. The choice of material was primarily governed by a required operating temperature exceeding 300 °C. Applications for HTSMAs, such as in operational chevrons [22] in the core region of a jet engine or for down-hole drilling requirements, primarily necessitate knowledge of the work capabilities of the HTSMA actuators. Earlier work has shown this alloy composition to produce recoverable strains up to approximately 3.0 % under zero load [11]. However there are no studies performed on the actuation response of the material under non-zero stress conditions and under multiple actuation cycles. The purpose of this work is to study in detail the effect of actuation stress and maximum applied strain levels on the actuator performance as well as the cyclic actuation behavior of the material.

The paper is organized as follows: Section 2 describes alloy fabrication and the experimental setup. The experimental procedure and the experimental results are presented in Section 3. The first part of section 3 deals with evaluation of the effect of maximum applied strain and actuation stress levels on the actuation behavior of the material under compression testing. The second part of section 3 deals with the actuation behavior under cyclic loading; discussion of the results follows in Section 4 and conclusions are given in Section 5.

2. FABRICATION AND EXPERIMENTAL SETUP

An ingot of a $Ti_{50}Pd_{40}Ni_{10}$ was cast by vacuum arc technique by melting individual metals of purity 99.99% Ti, 99.95% Pd and 99.99% Ni in a water-cooled copper hearth. The ingot was re-melted 3-4 times and homogenized at 1000 °C for 18ks. The cast bar was then hot rolled at 900 °C with a total thickness reduction of 30%, carried out in multiple steps. Samples of the material from both before and after rolling were cut using a low speed diamond saw and analyzed in a Pyris 1 DSC to determine the transformation temperatures. Figure 2 shows the transformation temperatures for both the as-cast and the rolled specimen. It is noticed that the rolled specimen shows a widening in the martensitic transformation range while the separation between the two transformation peaks was reduced considerably with the martensitic start temperature increasing by approximately 15 °C. If the precipitates were Ni or Pd-rich the transformation temperatures would be expected to increase or decrease, respectively. Since all the transformation temperatures except M_s show no substantial change after the rolling process, the precipitates may not be nickel or palladium rich. The precipitate may possibly be Ti rich oxides that could have formed during the hot rolling process (Figure 3). The increase in the M_s temperature may then be due to the precipitation caused during the hot rolling process. The exact composition of the precipitate was not determined in this study. After rolling, Electrode Discharge Machining (EDM) was used to fabricate cylindrical compression specimens.

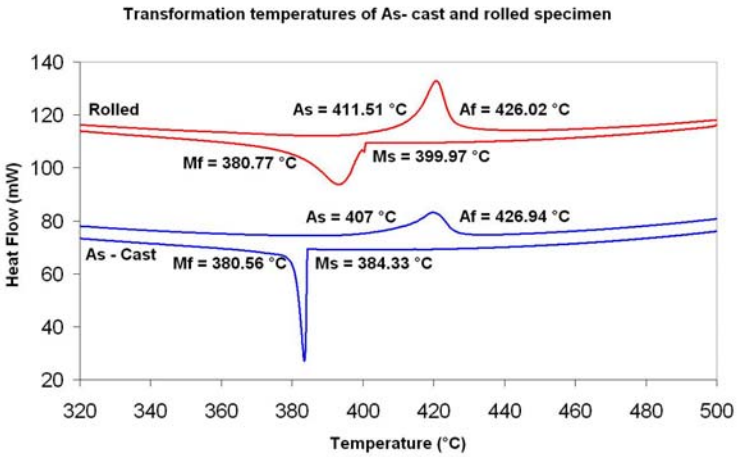

Figure 2. DSC graph showing transformation temperatures for the as cast and the rolled NiTiPd sample.

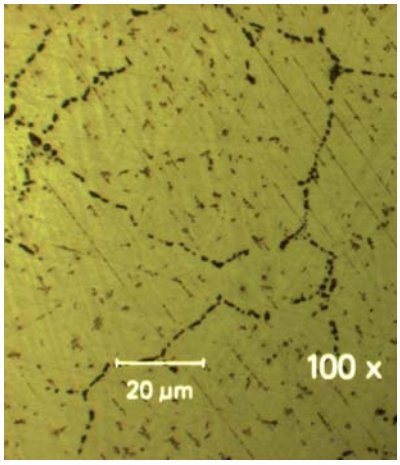

Figure 3. Micrograph of rolled specimen showing precipitation in the matrix.

A high temperature test system was developed for testing compression samples at temperatures ranging from room temperature (22 °C) to 600 °C. The grips used in the setup were made out of precipitation hardened Inconel (Inconel 718

AMS 5663) to avoid effects of softening of the grips. The top grip was water-cooled to prevent excessive thermal expansion during the heating process. The bottom grip rested on a steel plate, which supported the furnace and dissipated heat from the bottom grip. The furnace (Model E4 Quad elliptical heating chamber) and the extensometer (MTS 632.59B-01) were water-cooled to avoid overheating of these components during testing. The ceramic leads of the high temperature extensometer were spring loaded on the grips and held in position by friction. Figure 3 shows the experimental setup used for testing.

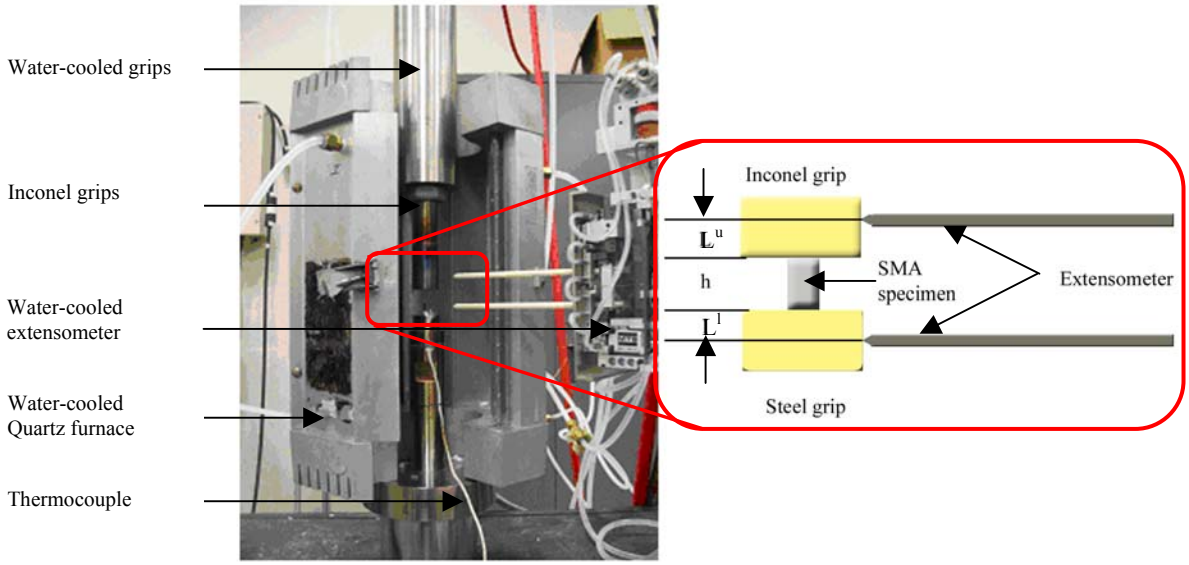

Figure 3. Experimental setup used for testing HTSMA showing water-cooled compression grips, extensometer and water-cooled quartz furnace.

During the setup the specimen was placed at the axial center of the bottom grip and a small pre-stress of 5 MPa was applied on the specimen by the top grip to avoid any slack effects due to imperfect contact. The temperature in the furnace was controlled using a high temperature thermocouple that touched the specimen surface. During varying temperature experiments, it was necessary that the temperature be varied slowly such that the system stabilized to a uniform specimen temperature. Stabilization was determined by monitoring the evolution in the strain.

3. EXPERIMENTAL PROCEDURE AND RESULTS

3.1 – Effect of actuation stress and maximum applied strain on recoverable strain

To design an SMA actuator, it is important to understand the effects of applied strain, actuation stress level and amount of recoverable strain under various loading conditions. A set of experiments were performed to evaluate the effects of these parameters. For an SMA actuator to operate effectively it is necessary to pre-strain the material before actuation under a certain load level. Figure 4 shows an actuation loading path illustrated on a stress-temperature phase diagram. The same loading path is shown in stress-strain diagram in Figure 5. The specimen was first heated to the test base temperature of 315 °C and allowed to stabilize before the test commenced. The specimen was detwinned (pre-strained) to a specific maximum applied strain level by an axial compressive load (represented by the loading path AB, Figure 4 and 5). On reaching B, the sample was unloaded to an actuation stress level (C) under which the material would be actuated by heating. At this point the stress on the sample was held constant and the strain was monitored as the sample was heated up to ten degrees above austenitic finish temperature (for the specific actuation stress level) and held there until the strain stabilized (D). Once the strain no longer changed, the sample was cooled to test base temperature (E). This completed one isobaric actuation cycle on the specimen. After the strain stabilized at the test base temperature the sample was unloaded to stress of 5 MPa (F). The specimen was then heated to above A_f (Point G) in order to recover any remnant detwinned martensite and then cooled to test base temperature (H). This step is essential to ensure completely

twinned martensite, especially if the actuation stress level (C) was above the detwinning stress level. This experiment was repeated by varying maximum applied strain and the actuation stress level, which are the control variables in this study. Figure 6 shows the strain temperature response of the material under actuation stress levels of 100 and 200 MPa with a maximum applied strain of 4.0%.

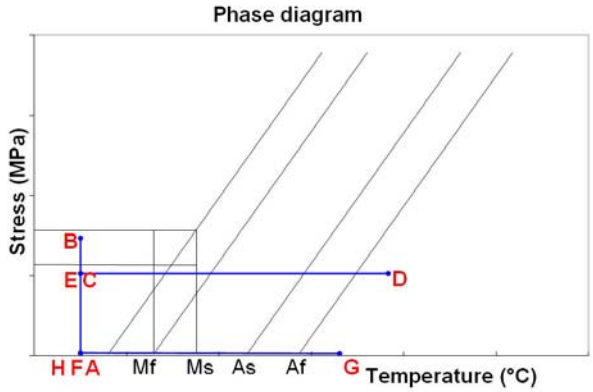

Figure 4. Phase diagram showing the detwinning followed by actuation under a constant stress level. Loading path ABCDEFGH.

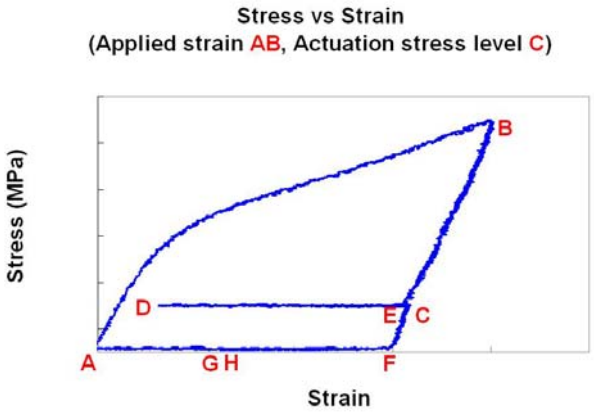

Figure 5. Stress-strain diagram showing the loading path ABCDEFGH and transformation strain recovery under stress level C.

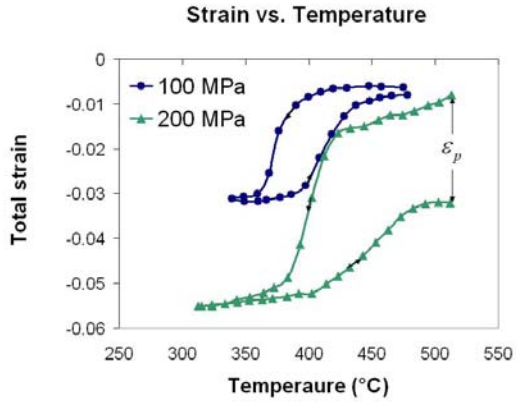

Figure 6. Strain-temperature for actuation stress levels of 100 and 200 MPa.

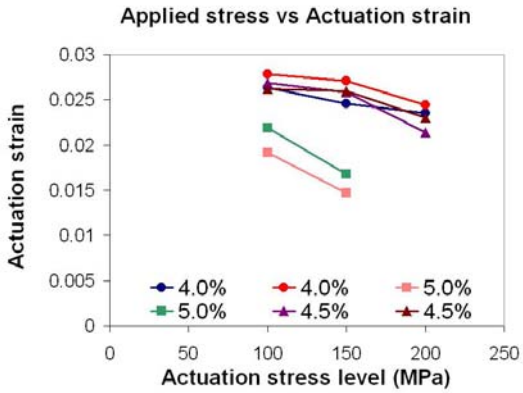

Figure 7. Transformation strain obtained under different actuation stress levels for different applied strains.

The strain indicated in the Figure 6 is the recorded total strain (from the extensometer). This strain includes the strain due to transformation, thermal expansion and elastic strain due to the applied stress. In order to obtain the exact recovered actuation strain (due to transformation) it is necessary to subtract the strains due to thermal expansion and elastic strain (due to applied stress) from the total recorded strain (ε_{ext}). These effects are subtracted from the recorded strain to obtain the recoverable strain (ε_t^{SMA}) due to SMA as shown in equation (1).

$$\varepsilon_t^{SMA} = \frac{1}{h}\left[\varepsilon_{ext}(L^u + h + L^l) - (L^u\alpha_u\Delta T + h\alpha_h\Delta T + L^l\alpha_l\Delta T + \frac{\sigma_{act}}{E_M^{SMA}}h)\right] \quad (1)$$

α_u, α_l, and α_h are the thermal expansion coefficients of the top grip, bottom grip and the SMA (h) respectively over a temperature range of ΔT. L^u and L^l represent the length of the top and the bottom grip respectively within the gauge length of the extensometer. E_M^{SMA} is the elastic modulus of the martensitic SMA (since the material is loaded in the martensitic state), and σ_{act} is the actuation stress level. It must be noted that in the tests performed, the applied strain is such that it results to a strain on the SMA of 4.0%. Figure 7 shows the recoverable strains obtained under different combinations of the control parameters (maximum applied strain and actuation stress level).

3.2 – Effect of multiple actuation cycles

The effect of repeated actuation cycles was also studied. In this study, the specimens were detwinned with 4.0 % maximum applied strain and unloaded to an actuation stress level of 100 MPa. The stress on the specimen was held constant and the strain was monitored while the specimen was taken through a complete thermally induced transformation cycle. The specimen was then unloaded and heated to recover any remnant detwinned martensite. The next cycle was started at that point. The cyclic actuation study of the specimen thus consisted of 10 actuation cycles at an actuation stress level of 100 MPa with consecutive unloading and recovery by heating. The stress-strain behavior of the material for multiple actuation cycles is shown in Figure 8. The evolution of the recoverable strain and the inelastic strain (unrecoverable strain at zero stress) with the number of cycles are shown in figures 9 and 10. DSC analysis was conducted on the specimen before and after cyclic loading and the transformation temperatures for both cases were compared. The transformation temperatures of the specimen before and after multiple cyclic actuations are shown in Figure 11.

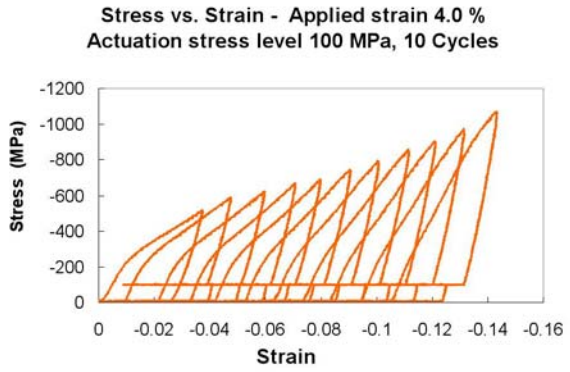

Figure 8. Stress-strain graph showing repeated actuation for 10 cycles.

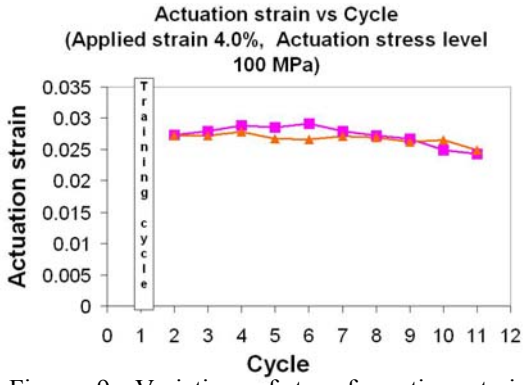

Figure 9. Variation of transformation strain with number of cycles for specimen cyclically actuated for 10 cycles.

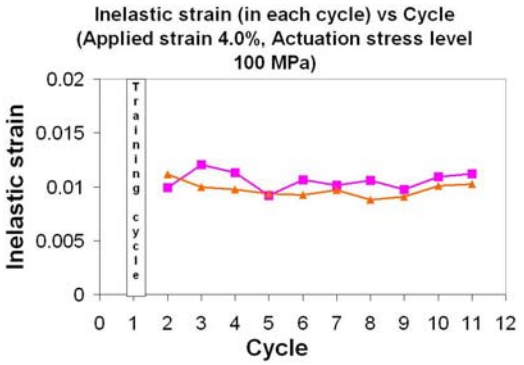

Figure 10. Plastic strain at the end of each stress-strain cycle for 10 cycles.

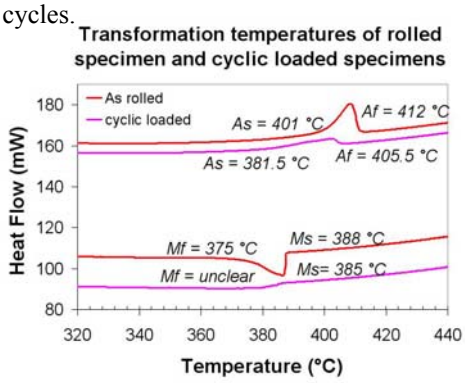

Figure 11. DSC curve of cyclic loaded specimen showing decrease and widening in the transformation temperatures when compared to the rolled specimen.

4. DISCUSSION

4.1 – Effect of actuation stress and maximum applied strain on recoverable strain

Figure 6 shows the strain-temperature diagram with the first cycle response under 100 and 200 MPa stress levels. It is noticed that at 100 MPa a large hysteresis with almost completely recoverable strain is obtained. However under the stress level of 200 MPa, higher inelastic strains are generated. It is possible that the increased stress level may have shifted the transformation temperatures to exceed the recrystallization temperatures resulting in loss of the elastic stored energy that drives the recoverable transformation strain. This hypothesis is supported by the work done by Xu et al. [19]. The variation of transformation strain with the different applied strain and actuation stress levels is shown in Figure 7. From this figure it is observed that the transformation strain reaches a maximum of 2.8 % with a 4.0 % applied strain and recovery at 100 MPa stress level. This is the highest observed transformation strain at 100 MPa for this material. With increasing actuation stress levels, the recoverable strain decreases to approximately 2.2 % at 200 MPa. With the 4.0 % and 4.5 % applied strain levels the specimens show good strain recovery under actuation stress levels of 100 MPa and 150 MPa, but the strain recovery diminishes rapidly at 200 MPa. It is also observed that with a 5.0 % applied strain the transformation strain in the material decreases rapidly. After a 5.0 % maximum applied strain, specimen testing at 200 MPa was aborted due to observable macroscopic plastic deformation. This may be due to the excessive plastic strain accumulated in the previous cycles (100 MPa and 150 MPa).

The energy density of the actuator subject to a 4.0 % maximum applied strain and a 100 MPa and 200 MPa constant actuation stress levels are calculated to be approximately 431 J/Kg and 744 J/Kg respectively. These values are lower than the energy density of conventional Nitinol SMA, which shows an energy density of approximately 1KJ/Kg. However the energy density is much higher than that of most conventional active materials [23] with the key benefit of $Ti_{50}Pd_{40}Ni_{10}$ having the ability to operate at high temperatures of 300-500 °C.

4.2 – Effect of multiple actuation cycles

From Figure 8 it is observed that there is a distinct increase in hardening that accompanies the detwinning process and there is no stabilization in hardening observed for 10 continuous cycles. From these tests, it is also observed that the specimen is capable of producing consistent transformation strains for 10 cycles (Figure 9). Figure 10 also shows the inelastic strain accumulation generated in each cycle. It is noted that with every cycle the specimen generate approximately the same amount of inelastic strain (1.0 %) for the 10 actuation cycles. This inelastic strain may be due to the hardening behavior observed in each cycle during detwinning. The effect of cyclic deformation is well observed in the DSC results, which show a widening is the transformation curve and a decrease in the transformation temperatures in the cyclic loaded specimen. This may be attributed to the high precipitate density that results in suppressing the reverse transformation and thus causing a decrease in the transformation temperatures. This behavior is similar to the cyclic behavior response observed in Nitinol SMAs [24].

5. SUMMARY AND CONCLUSIONS

A detailed thermomechanical experimental study was performed on the $Ti_{50}Pd_{40}Ni_{10}$ specimens to understand the materials performance as an actuator. The effect of different actuation stress levels and multiple actuation cycles on the recoverable actuation strain has been investigated in this material. Recoverable strain of 2.2 – 2.8% was observed under constant applied stress levels of 100 – 200 MPa. It was also noticed that the actuation strain in the material decreases with increasing maximum applied strain or actuation stress. Finally cyclic loading behavior indicated consistent performance of the material for 10 cycles.

ACKNOWLEDGMENTS

The authors acknowledge the valuable contributions in experimental work by Brent Volk and Darren Hartl.

REFERENCES

1. A. Srinivasan, D. McFarland, "Smart Structures: Analysis and Design", Cambridge University Press, Cambridge, 2001.
2. K. Otsuka, C. M. Wayman, "Shape Memory Materials", Cambridge University Press, Cambridge, 1999.
3. H. E. Karaca, I. Karaman, D. C. Lagoudas,H. J. Maier and Y.I. Chumlyakov, "Recoverable stress-induced martensitic transformation in a ferromagnetic CoNiAl alloy", Scripta Materialia, Vol. 49, no. 9, 831-836, 2003.
4. H. Funakubo, "Shape Memory Alloys", Gordon and Breach Science Publishers, 1984.
5. N. B. Morgan, "Medical shape memory alloy applications-the market and its products", Materials science and engineering A 378, 16-23, 2004.
6. P.G. Lidquist and C.M. Wayman, "Shape memory and transformation behavior of martensitic Ti-Pd-Ni and Ti-Pt-Ni alloys, Engineering Aspects of Shape Memory Alloys", Ed. T. W. Duerig, K. N. Melton, D. Stöckel and C. M. Wayman, Butterworth-Heinemann, London, 129, 1990.
7. P. E. Thoma and J. J. Boehm, "Effect of composition on the amount of second phase and transformation temperatures of NixTi90-xHf10 shape memory alloys", Materials science and engineering A 273-275, 385-389, 1999.
8. K. Otsuka, X. Ren, "Recent developments in the research of shape memory alloys", Intermetallics 7, 511-528, 1999.
9. G.S. Firstov, J. Van Humbeecka, Y.N. Koval, "High-temperature shape memory alloys-Some recent developments", Materials Science and Engineering A 378, 2–10, 2004.
10. K. Otsuka, K Oda, Y. Ueno and Min Piao, "The shape memory effect in a $Ti_{50}Pd_{50}$ alloy", Scripta Metallurgica et Materialia, Vol. 29, 1355-1358, 1993.
11. D. Goldberg, Y. Xu, Y. Murakami, K. Otsuka, T. Ueki and H. Horikawa, High-temperature shape memory effect in Ti50Pd50-xNix (x=10, 15, 20) alloys, Materials letters 22, 241-248, 1995.
12. E. P. George, C. T. Liu, J. A. Horton, C. J. Sparks* M. Kao, H. Kunsmann and T. King. "Characterization, Processing, and Alloy Design of NiAI-Based Shape Memory Alloys", MATERIALS CHARACTERIZATION 32, 139-160, 1994.
13. T. Cheng, "High Temperature Shape Memory Effects of Ni-34.6at%Al with improved ductility and toughness", Scripta Metallurgica et Materialia, Vol. 31, No. 9, 1187-1192, 1994.
14. S. Shimizu, Y. Xu, E. Okunishi, S. Tanaka, K. Otsuka and K. Mitose, Improvement of shape memory characteristics by precipitation hardening of Ti-Pd-Ni alloys, Materials letters 34, 23-29, 1998.
15. Q. Tian, J. Wu and C. Xie, "The superelasticity and Microstructure of $Ti_{50+x}Pd_{30}Ni_{20-x}$ High - temperature Shape Memory Alloys", Proceeding of SPIE Vol. 4333, 2001.
16. J. Wu and Q. Tian, "The superelasticity of TiPdNi high temperature shape memory alloy", Intermetallics 11, 773-778, 2003.
17. D. Goldberg, Y. Xu, Y. Murakami, S. Morito, K. Otsuka, T. Ueki and H. Horikawa, "Characterization of Ti50Pd30N20 high-temperature shape memory alloy", Intermetallics 3, 35-46, 1995.
18. W. Cai and K. Otsuka, "Martensitic aging effect in a Ti50Pd50 high temperature shape memory alloy", Scripta Materialia, Vol. 41, No. 12, 1311-1317, 1999.
19. Ya. Xu, K. Otsuka, E. Furubayashi and K. Mitose, "TEM observeation of recrystallization process in solution-treated Ti50Pd50 martensite", Material letters 34, 14-18, 1998.
20. W. Cai, K. Otsuka and M. Asai, "Martensitic aging effect in Ti-Pd and Ti-Pd-Ni high temperature shape memory alloys", Materials transactions, JIM, vol. 40, No. 9, 895-898, 1999.
21. Ya. Xu, S. Shimizu, Y. Suzuki, K. Otsuka, T. Ueki and K. Mitose, "Recovery and recrystallization processes n Ti-Pd-Ni high temperature shape memory alloys", Acta Metallurgica, 1997.
22. F. T. Calkins, G.W. Butler, "Subsonic Jet Noise Reduction Variable Geometry Chevron, 42nd Aerospace Sciences Meeting and Exhibit, 2004.
23. J. D. W. Madden, N. A. Vandesteeg, P. A. Anquetil, P. G. A. Madden, A. Takshi, R. Z. Pytel, S. R. Lafontaine, P. A. Wieringa, and I. W. Hunter, "Artificial Muscle Technology: Physical Principles and Naval Prospects", IEEE Journal of oceanic engineering, Vol. 29, No. 3, 706-727, 2004.
24. S. Miyazaki, Y. Igo and K. Otsuka, "Effect of thermal cycling on the transformation temperatures of Ti-Ni alloys", Acta Metallurgica, Vol. 34, No. 10, 2045-2051, 1986.